pISSN 2384-1095
eISSN 2384-1109

iMRI 2015;19:212-217

http://dx.doi.org/10.13104/imri.2015.19.4.212

iMRI
Investigative Magnetic Resonance Imaging

Determination of Optimal Scan Time for the Measurement of Downstream Metabolites in Hyperpolarized ^{13}C MRSI

Hansol Lee[1], Joonsung Lee[2], Eunhae Joe[1], Seungwook Yang[1], Young-suk Choi[3], Eunkyung Wang[3], Ho-Taek Song[3], Dong-Hyun Kim[1]

[1]Department of Electrical & Electronic Engineering, Yonsei University, Seoul, Korea
[2]Center for Neuroscience Imaging Research, Institute for Basic Science, Sungkyunkwan University, Gyeonggi-do, Korea
[3]Department of Radiology, Yonsei University College of Medicine, Seoul, Korea

Original Article

Received: June 23, 2015
Revised: September 3, 2015
Accepted: September 10, 2015

Correspondence to:
Dong-Hyun Kim, Ph.D.
Department of Electrical & Electronic Engineering, Yonsei University, Yonsei-ro 50, Seodaemun-gu, Seoul 03722, Korea.
Tel. +82-2-2123-5874
Fax. +82-2-313-2879
Email: donghyunkim@yonsei.ac.kr

Purpose: For a single time-point hyperpolarized ^{13}C magnetic resonance spectroscopy imaging (MRSI) of animal models, scan-time window after injecting substrates is critical in terms of signal-to-noise ratio (SNR) of downstream metabolites. Pre-scans of time-resolved magnetic resonance spectroscopy (MRS) can be performed to determine the scan-time window. In this study, based on two-site exchange model, protocol-specific simulation approaches were developed for ^{13}C MRSI and the optimal scan-time window was determined to maximize the SNR of downstream metabolites.
Materials and Methods: The arterial input function and conversion rate constant from injected substrates (pyruvate) to downstream metabolite (lactate) were pre-calibrated, based on pre-scans of time-resolved MRS. MRSI was simulated using two-site exchange model with considerations of scan parameters of MRSI. Optimal scan-time window for mapping lactate was chosen from simulated lactate intensity maps. The performance was validated by multiple *in vivo* experiments of BALB/C nude mice with MDA-MB-231 breast tumor cells. As a comparison, MRSI were performed with other scan-time windows simply chosen from the lactate signal intensities of pre-scan time-resolved MRS.
Results: The optimal scan timing for our animal models was determined by simulation, and was found to be 15 s after injection of the pyruvate. Compared to the simple approach, we observed that the lactate peak signal to noise ratio (PSNR) was increased by 230%.
Conclusion: Optimal scan timing to measure downstream metabolites using hyperpolarized ^{13}C MRSI can be determined by the proposed protocol-specific simulation approaches.

Keywords: Hyperpolarized ^{13}C; MRSI; Two-site exchange; Pyruvate; Lactate

INTRODUCTION

Hyperpolarized ^{13}C magnetic resonance spectroscopy imaging (MRSI) is an emerging technique to observe the metabolic activities of tissue after injecting hyperpolarized ^{13}C-labeled substrates (1, 2). Due to a low natural abundance of ^{13}C, a special technique and equipment (dynamic nuclear polarization [DNP]), are required to enhance the

magnetic sensitivity of ^{13}C nuclei by 10,000-fold or more, compared to the thermal equilibrium (3). One of the widely used molecules for hyperpolarization is [1-^{13}C] pyruvate, which is converted to several downstream metabolites such as lactate, alanine, and bicarbonate (4). The real time metabolic activities of tissues can be observed by measuring the conversion of injected substrate to downstream metabolites via magnetic resonance spectroscopy (MRS). Diagnosis and observation of treatment response for several diseases, such as cancer (2, 5, 6), heart disease (7), and diabetes (8), can be made by observation of metabolic activities.

Hyperpolarized ^{13}C-labled substrates experience irrecoverable signal decay by T1 relaxation. With T1 relaxation constraint of ~20 s (9.4 T), it is important to acquire the hyperpolarized signal rapidly and efficiently. Furthermore, downstream metabolites converted from injected substrates still have a low sensitivity. Thus, it is critical to determine optimal scan-time window to increase the signal-to-noise ratio (SNR) in hyperpolarized ^{13}C MRSI. Conventionally, pre-scans of time-resolved hyperpolarized ^{13}C magnetic resonance spectroscopy (MRS) were performed, and the scan-time window was determined directly from the dynamic intensity curves of downstream metabolites (9); however, this approach may not be optimal. In pre-scans of time-resolved MRS, RF excitations were performed before, or right after, injection of pyruvate. However, in hyperpolarized ^{13}C MRSI, RF excitation were performed only during the pre-determined scan-time window. Due to different RF excitations, and thus the different remaining polarizations, dynamic polarization curves in hyperpolarized ^{13}C MRSI cannot be represented well by the dynamic intensity curves in time-resolved MRS. In this study, the protocol-specific simulation methods using two-site exchange model were proposed to find the optimal scan-time window to maximize the SNR of downstream metabolites in hyperpolarized ^{13}C MRSI. Determined optimal scan-time window was validated by multiple *in vivo* experiments of tumor-bearing mice via injection of hyperpolarized [1-^{13}C] pyruvate.

MATERIALS AND METHODS

MRSI Simulation Based on Two-site Exchange Model

The dynamic curve of pyruvate and lactate signal can be simulated by considering the arterial input function (AIF) of the two-site exchange model, i.e., Eq. [1-2] (10).

$$M_{pyr}(t)=\begin{cases}\dfrac{rate_{inj}}{k_{pyr}}\left(1-e^{-k_{pyr}(t-t_{arr})}\right), & t_{arr}\le t<t_{end}\\ M_{pyr}(t_{end})\,e^{-k_{pyr}(t-t_{end})}, & t>t_{end}\end{cases} \quad [1]$$

$$M_{lac}(t)=\begin{cases}\dfrac{k_{pyr\to lac}\,rate_{inj}}{k_{pyr}-k_{lac}}\left(\dfrac{1-e^{-k_{lac}(t-t_{arr})}}{k_{lac}}-\dfrac{1-e^{-k_{pyr}(t-t_{arr})}}{k_{pyr}}\right), & t_{arr}\le t<t_{end}\\ \dfrac{M_{pyr}(t_{end})\,k_{pyr\to lac}}{k_{pyr}-k_{lac}}\left(e^{-k_{lac}(t-t_{end})}-e^{-k_{pyr}(t-t_{end})}\right)+M_{lac}(t_{end})\,e^{-k_{lac}(t-t_{end})}, & t\ge t_{end}\end{cases} \quad [2]$$

Here, $M_{pyr}(t)$ and $M_{lac}(t)$ are the time course function of ^{13}C pyruvate and lactate signal, respectively. In addition, several parameters are used for this model. k_x (x represents the pyruvate or lactate) is the rate constant for signal decay (in s^{-1}), which involves both T_1 decay and signal loss from excitation. $k_{pyr\to lac}$ represents the conversion rate constant (in s^{-1}). $rate_{inj}$ is the rate of pyruvate arrival (in a.u. s^{-1}). t_{arr} represents the time of pyruvate arrival (in s), and t_{end} is the time of pyruvate maximum in the dynamic curve (in s). In this simulation model, several assumptions were made. First, duration from t_{arr} to t_{end}, rate of injection ($rate_{inj}$), the T_1 relaxation time of pyruvate, and conversion rate constant of pyruvate to lactate ($k_{pyr\to lac}$) for selected slice, can be estimated by pre-scans of time-resolved MRS. Second, the T_1 relaxation times of pyruvate and lactate are equal (2). Backward reaction rate constant ($k_{lac\to pyr}$) was ignored (6). Based on the pre-scans, the parameters used for simulation are as follows; 6s of duration between t_{arr} and t_{end}, 0.3 s^{-1} of $rate_{inj}$, 21 s of T_1 for 9.4 T *in vivo* environments, 0.0063 s^{-1} of $k_{pyr\to lac}$.

Based on the dynamic curve simulation, signal intensities of lactate on MRSI were simulated with multiple conversion rate constant values ($k_{pyr\to lac}$) and starting time of MRSI after injection (time after t_{end}). The parameters of MRSI simulation are 10° of flip angle, 21 s of T1 relaxation time, 81ms of repetition time (TR), and 8 × 8 matrix size. Other parameters were the same as the dynamic curve simulation.

In vivo Experiments

All experiments were performed on a 9.4 T Bruker BioSpec 94/20 small animal imaging MRI (Bruker BioSpin MRI GmbH, Ettlingen, Germany) equipped with ^{1}H-^{13}C dual-tuned mouse surface transmit/receive coil. Six-weeks-old BALB/C nude mice, with MDA-MB-231 breast tumor cells implanted in the striatum of brain, were used for the animal studies. The mice were anesthetized using isoflurane during the MRI scan at the level of 1-3%. The animals were

kept warm on a heating bed with circulating warm water. Temperature and breathing were monitored during the experiments. All animal procedures were approved by the institute animal care and use committee. For anatomical information, high resolution T_2-weighted turbo RARE ^{1}H MR images in axial plane were acquired, with 2 mm slice thickness and 0.125 × 0.125 mm^2 resolution.

For hyperpolarized ^{13}C experiments, [1-^{13}C] pyruvic acid doped with 15 mM Trityl radical and 1.5 M Dotarem was polarized using HyperSense DNP polarizer (Oxford Instruments, Molecular Biotools, Oxford, UK). 3.8 mL of Tris/EDTA (40 mM Tris, 21.6 mM NaOH, 0.1 g/L EDTA, 50 mM NaCl) solution was used for dissolution. After dissolution, approximately 350 µl of hyperpolarized pyruvate, having a concentration of 75 mM and a pH of around 7.5, was injected over a duration of 6 s, through a tail vein catheter.

For time-resolved hyperpolarized ^{13}C MRS experiments, slice-selective FID data with a flip angle of 10° and temporal resolution of 1 s were acquired using a pulse and acquire sequence. A 10 mm-thick axial slice was selected, including whole brain. Data acquisitions started before the injection of [1-^{13}C] pyruvate into mouse and continued for two minutes. The spectral bandwidth of acquired data was 6510 Hz with 2048 spectral points. Seventeen BALB/C nude mice, having the MDA-MB-231 breast tumor cells, were scanned.

For hyperpolarized ^{13}C MRSI experiments, FID CSI sequence with centric-ordered phase encoding was used. MRSI data were acquired with constant flip angle (FA = 10°), repetition time (TR = 81 ms), and 2 mm of slice thickness, resulting in a total scan time of 5.2 s. The FOV was set to 16 × 16 mm^2 to cover a mouse brain having 8 × 8 matrix size. The spectral bandwidth of acquired data was 6510 Hz with 512 spectral points. Hyperpolarized ^{13}C MRSI experiments were performed at different scan timing to compare the SNR of downstream metabolites on targeted tumor between, before, and after optimization (n = 3 for 7 s after injection, and n = 3 for 15 s after injection).

All data were processed using MATLAB (R2012a, MathWorks, Natick, MA, USA). MRS and MRSI data were apodized by a 33 Hz Lorentzian filter and zero-padded with 4096 points in time domain prior to FFT. The conversion rate constant, $k_{pyr\rightarrow lac}$, was estimated from pre-scans of time-resolved MRS data by fitting the dynamic intensity curves to Eq. [1] and [2] after injection ($t > t_{end}$). The metabolite map was obtained from MRSI data by measuring the peak signal-to-noise ratio (PSNR) values of metabolites in each voxel. To visualize the results, measured PSNR values were overlaid with the high resolution ^{1}H T_2-weighted anatomical image.

RESULT

In time-resolved MRS, the apparent conversion rate constant was estimated as 0.0063 ± 0.004 in selected tumor-bearing slices (n = 17). In addition, T_1 relaxation time constant was estimated at 21 ± 4.4 s in 9.4 T environments.

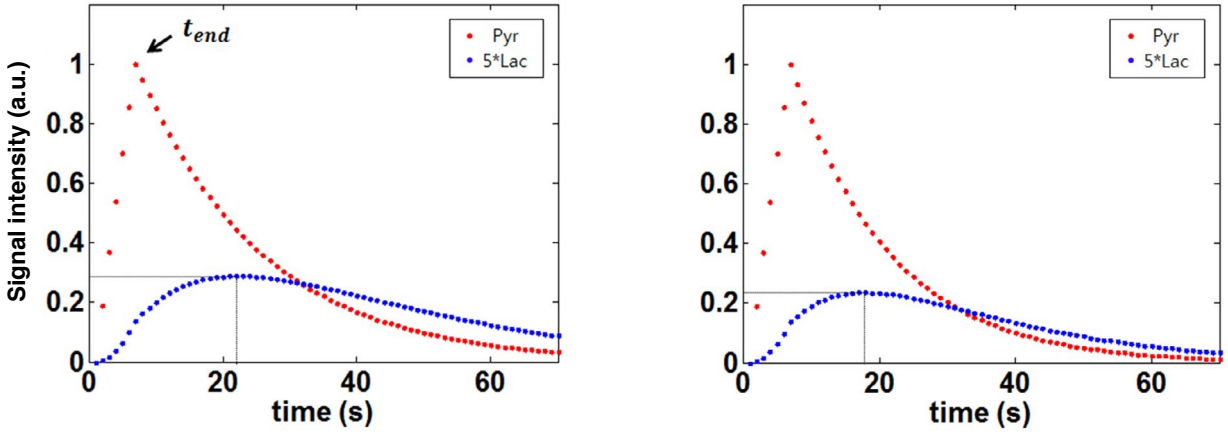

a b

Fig. 1. Simulation of two-site exchange model (a) without and (b) with RF excitation of FA = 10°. Temporal resolution for two-site exchange simulation was 1 s ($k_{pyr\rightarrow lac}$ = 0.0063 s^{-1}, T_1 = 21 s). In simulated dynamic curve, peak of the lactate signal appeared (a) 22 s and (b) 18 s after pyruvate arrival, respectively.

Mean values of apparent conversion rate constant and T_1 relaxation time constant were used for determining the optimal scan-time window for hyperpolarized ^{13}C MRSI.

Figure 1 represents the simulated lactate signal with temporal resolution of 1 s for two cases, one without RF excitation (Fig. 1a) and one with RF excitation (flip angle = 10°) (Fig. 1b). In simulated lactate signal evolution without RF excitations (Fig. 1a), lactate has maximum signal intensity at 16 s after t_{end}, which is 22 s after pyruvate arrival (red dotted line). With RF excitations, maximum of lactate signal appeared 18 s after pyruvate arrival (Fig. 1b), which is 4 s earlier than without RF excitation.

In addition to previous dynamic simulation, the signal intensities of lactate on MRSI were simulated with multiple conversion rate constant values in ranges of 0.001-0.02 and acquisition timings in range of 0-30 s (Fig. 2). The optimal scan timing for any conversion rate constant, which results in the maximum signal intensity of lactate on MRSI, can be determined by simulation (Fig. 2a). Figure 2b shows the optimal scan timing for each $k_{pyr\rightarrow lac}$. For higher conversion rate constant, the optimal scan timing is earlier. The optimal scan timing corresponding to the measured mean apparent conversion rate constant was about 15 s after injection. Figure 2c compares the lactate signal intensity acquired at different scan timing for each $k_{pyr\rightarrow lac}$: optimal timing, 7 s after t_{end} and 15 s after t_{end}. For 0.0063 of $k_{pyr\rightarrow lac}$, the lactate signal intensity acquired at 7 s after t_{end} is 10% less than the optimal timing. In contrast, the lactate signal intensity scanned at 15 s after t_{end} is 0.01% less than optimal timing. Thus, we can say that the optimal scan time is almost 15 s

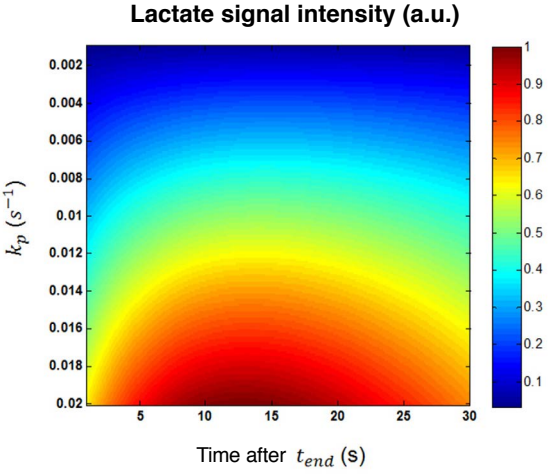

a

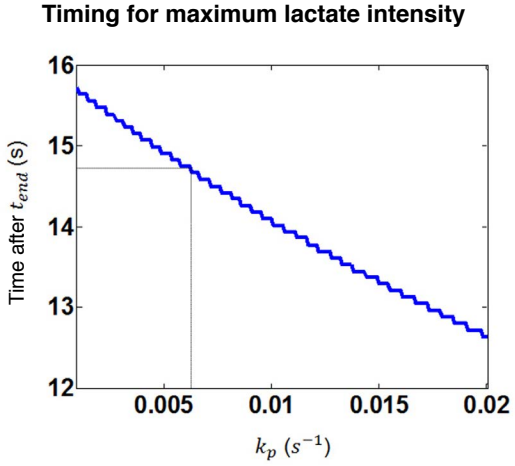

b

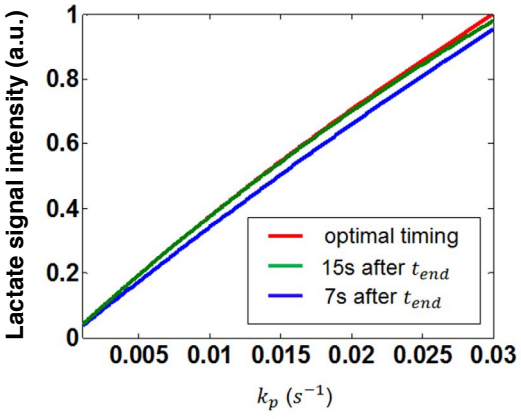

c

Fig. 2. (a) Simulated lactate signal intensities in hyperpolarized ^{13}C MRSI based on two-site exchange model with multiple $k_{pyr\rightarrow lac}$ values and acquisition timing with FA = 10°, T1 = 21 s. (b) The optimal scan timing for each $k_{pyr\rightarrow lac}$. The optimal scan time for the estimated $k_{pyr\rightarrow lac}$, 0.0063, was about 15 s after t_{end}. (c) The lactate signal intensities in MRSI with different scan timings; optimal timing (red line), 7 s after t_{end} (blue line), and 15 s after t_{end} (green line). For estimated $k_{pyr\rightarrow lac}$ value of 0.0063, lactate signal intensity acquired at 7 s after t_{end} was 10% less than optimal timing. The lactate signal intensity acquired at 15 s after t_{end} was 0.01% less than optimal timing.

after t_{end}.

For *in vivo* experiments, multiple hyperpolarized ^{13}C MRSI were performed to compare the SNR of lactate between, before, and after optimization of scan timing. Control experiments were performed by scanning at the earlier timing of 7 s after t_{end}. Figure 3 shows the lactate peak signal-to-noise (PSNR) maps. Before the optimization of scan-time window, PSNR of lactate in the voxels corresponding to tumor was 8 ± 4.6 (n = 3). PSNR of lactate scanned after optimization of scan-time window was 18.5 ± 3.1 (n = 3). Through the optimization of scan-time window using simulation of two-site exchange model, 230% increase in the downstream metabolite PSNR was achieved.

DISCUSSION

In this study, the measured conversion rate constant ($k_{pyr\rightarrow lac}$) value of selected tumor-bearing slice was very low (0.0063 s^{-1}). Due to a low concentration of lactate converted from the injected pyruvate, SNR of lactate signal in selected slice was low. The improvements in lactate SNR was achieved by optimization of scan-time window. For higher values of $k_{pyr\rightarrow lac}$, a higher increase in the lactate SNR can be expected (Fig. 2c).

In this study, the pre-scans of time-resolved MRS data were acquired from tumor-bearing slice, including normal brain. In other words, the acquired data represented the dynamics of both normal brain and tumor. Scan-time window was optimized to improve the SNR of lactate in whole slices. If the $k_{pyr\rightarrow lac}$ of tumor can be measured, the scan-time window can be optimized to improve SNR of lactate signal in tumor.

In pre-scans of time-resolved MRS, the standard deviation of estimated $k_{pyr\rightarrow lac}$ value was comparable to the mean value. The conversion rate constant depends on the progression of tumor, conditions of each mouse (perfusion, metabolism, and anesthesia state etc.), and conditions of experiments (hyperpolarization level, injection duration etc.). Mean value of estimated $k_{pyr\rightarrow lac}$ was used for simulation to optimize the scan-time window.

In hyperpolarized ^{13}C studies, the signal is irrecoverable, which decreases with metabolic conversion, T1 relaxation, and RF excitation. For these reasons, we used FID CSI sequence with centric ordered phase encoding. After acquiring data on the center of k-space first, it is beneficial to increase the SNR of metabolites. Furthermore, temporal and spatial resolutions are limited. Due to these limitations, low resolution of MRSI experiments, which were 2 × 2 mm^2 of resolution, were performed in this study. The PSNR of lactate in MRSI was calculated voxel by voxel as shown in

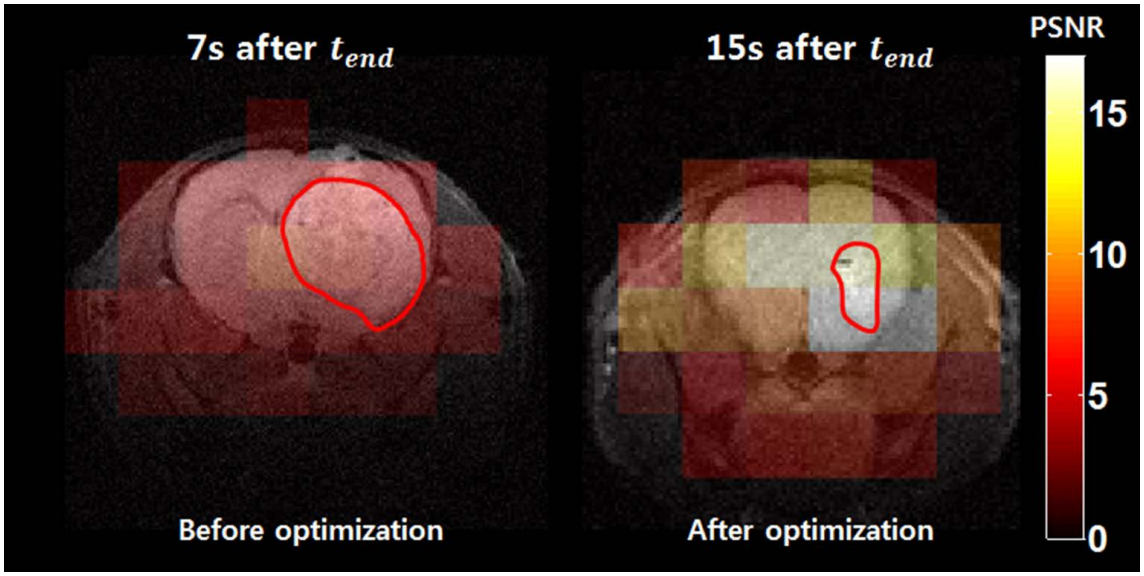

Fig. 3. Comparison of lactate map acquired at (a) control, 7 s after t_{end} and (b) optimized timing, 15 s after t_{end}, overlaid with ^{1}H anatomical image. The lactate map was obtained by measuring peak signal-to-noise ratio (PSNR) of lactate in each voxel. The PSNR corresponding tumor voxels was 8 ± 4.6 for 7 s after t_{end}, and 18.5 ± 3.1 for 15 s after t_{end} (n = 3 per measurement). The boundary of tumor implanted in mice brain is represented as a red line.

Figure 3. In low resolution images, partial-volume effects can lead to errors in the quantification of lactate in the brain and tumor tissues. If the MRSI experiments are performed with higher resolution, the quantification of PSNR improvement can be more accurate.

Furthermore, the lactate map was well-localized to the tumor after scan-time window optimization (Fig. 3). However, any quantitative analysis related to localization was not performed in this study. Localization analysis involved with simulating point spread functions (PSFs) remains as a future work.

In conclusion, in hyperpolarized ^{13}C MRSI experiments, it is important to determine the scan-time window in terms of SNR of downstream metabolites. Conventionally, the scan-time window was determined by pre-scans of time-resolved MRS experiments. However, it may not be an optimal timing. Thus, protocol-specific simulation approaches were developed to determine the optimal scan-time window for hyperpolarized ^{13}C MRSI. Using the determined optimal scan-time window, SNR of downstream metabolites (i.e., lactate) was maximized in hyperpolarized ^{13}C MRSI.

Acknowledgments

This work was financially supported by the Korean Health Technology R&D Project, Ministry for Health, Welfare & Family Affairs (A110035-1101-0000200).

REFERENCES

1. Golman K, Zandt RI, Lerche M, Pehrson R, Ardenkjaer-Larsen JH. Metabolic imaging by hyperpolarized ^{13}C magnetic resonance imaging for *in vivo* tumor diagnosis. Cancer Res 2006;66:10855-10860
2. Day SE, Kettunen MI, Gallagher FA, et al. Detecting tumor response to treatment using hyperpolarized 13C magnetic resonance imaging and spectroscopy. Nat Med 2007;13:1382-1387
3. Ardenkjaer-Larsen JH, Fridlund B, Gram A, et al. Increase in signal-to-noise ratio of > 10,000 times in liquid-state NMR. Proc Natl Acad Sci U S A 2003;100:10158-10163
4. Golman K, Zandt RI, Thaning M. Real-time metabolic imaging. Proc Natl Acad Sci U S A 2006;103:11270-11275
5. Darpolor MM, Yen YF, Chua MS, et al. *In vivo* MRSI of hyperpolarized [1-(13)C]pyruvate metabolism in rat hepatocellular carcinoma. NMR Biomed 2011;24:506-513
6. Harris T, Eliyahu G, Frydman L, Degani H. Kinetics of hyperpolarized ^{13}C1-pyruvate transport and metabolism in living human breast cancer cells. Proc Natl Acad Sci U S A 2009;106:18131-18136
7. Lau AZ, Chen AP, Ghugre NR, et al. Rapid multislice imaging of hyperpolarized ^{13}C pyruvate and bicarbonate in the heart. Magn Reson Med 2010;64:1323-1331
8. Schroeder MA, Cochlin LE, Heather LC, Clarke K, Radda GK, Tyler DJ. *In vivo* assessment of pyruvate dehydrogenase flux in the heart using hyperpolarized carbon-13 magnetic resonance. Proc Natl Acad Sci U S A 2008;105:12051-12056
9. Kohler SJ, Yen Y, Wolber J, et al. *In vivo* 13 carbon metabolic imaging at 3T with hyperpolarized ^{13}C-1-pyruvate. Magn Reson Med 2007;58:65-69
10. Zierhut ML, Yen YF, Chen AP, et al. Kinetic modeling of hyperpolarized ^{13}C1-pyruvate metabolism in normal rats and TRAMP mice. J Magn Reson 2010;202:85-92